



## Determination of the parameters of the firefly method for PID parameters in solar panel applications

**Machrus Ali<sup>1\*</sup>, Hadi Suyono<sup>2</sup>, Muhammad Aziz Muslim<sup>2</sup>, Muhammad Ruswandi Djalal<sup>3</sup>, Yanuar Mahfudz Safarudin<sup>4</sup>, Aji Akbar Firdaus<sup>5</sup>**

<sup>1</sup>Department of Electrical Engineering, Universitas Darul Ulum, Indonesia

<sup>2</sup>Department of Electrical Engineering, Universitas Brawijaya, Indonesia

<sup>3</sup>Department of Electrical Engineering, Politeknik Negeri Ujung Pandang, Indonesia

<sup>4</sup>Department of Electrical Engineering, Politeknik Negeri Semarang, Indonesia

<sup>5</sup>Department of Engineering, Universitas Airlangga, Indonesia

### Abstract

The optimal performance of solar panels is very important to produce maximum electrical energy. Solar panels can work optimally when equipped with a solar tracker. The solar panel tracker works by following the sun's movement. A Proportional, Integral, Derivative (PID) based control is used to optimize the performance of the solar tracker. An optimal tuning is needed to get the PID parameter. The Firefly method is an intelligent method that can be used to optimize PID parameters. Three Firefly Algorithm (FA) parameters are used in the program: Beta is used to determine firefly speed, Alpha is used for flexibility of movement, and Gamma is used for more complex constraints or problems. This Dual Axis photovoltaic tracking study uses the beta value determination, changing the Beta value from 0.1 to 0.9. From the results of 10 models, it was found that the PID constant values were varied. On the horizontal Axis, the best results are if the Beta is given at 0.4, and the worst result is if the Beta is given at 0.8. On the vertical Axis, the best results are if the Beta is given at 0.3, and the worst result is if the Beta is given at 0.8.

This is an open access article under the [CC BY-NC license](#)



### Keywords:

Dual Axis Tracking;  
Energy Conversion;  
Firefly Algorithm;  
Photovoltaic;

### Article History:

Received: October 8, 2021

Revised: December 28, 2021

Accepted: January 2, 2022

Published: June 15, 2022

### Corresponding Author:

Machrus Ali,  
Department of Electrical  
Engineering, Universitas Darul  
Ulum, Indonesia  
Email: [machrus7@gmail.com](mailto:machrus7@gmail.com)

## INTRODUCTION

Renewable energy is an alternative to replace fossil energy. Some of the renewable energy that is developing is photovoltaic and wind turbine. Photovoltaic is very promising to be developed into electrical energy [1, 2, 3, 4]. However, solar radiation makes the temperature less intermittent than the wind turbine's wind speed to produce electricity [5][6]. Several ways to overcome solar radiation and temperature have intermittent properties so that the PV output power can be maximized. One way is to use solar power tracking.

The sun tracking system is classified into one-track and two-axis solar tracking. The elevation angle is the angle of the sun's height measured from the horizontal direction. At sunrise or sunset, the elevation angle value is zero degrees [7][8].

The maximum elevation angle is 90° when the sun is directly above the head. The sun's azimuth angle is the position of the sun's angle measured from the north direction of the earth. The azimuth angle of the sun is 0° in the north, 90° in the east, and 180° in the south. A qualitative and quantitative comparison of the performance of a two-axis solar tracking photovoltaic system in terms of radiation and energy yield is better than a fixed position photovoltaic system based on the Malaysian climate environment. The study calculated a one-year increase in efficiency in the Azimuth-Altitude Dual Axis Solar Tracker compared to without a solar tracking system amounted to 48.98%, and efficiency increased by 36.504% in one year when compared to a single-axis solar tracker [9][10].

Some artificial intelligence has been developed to be able to find maximum PV power,

such as Neural Network (NN) [11], Particle Swarm Optimization [12], Gray Wolf Optimization (GWO), and Fuzzy Logic Controller [13][14]. However, PV power is still less than the maximum. In this paper, a two-axis solar tracking system or elevation angle and azimuth angle tracking is controlled by a PID (Proportional Integral Derivative) where the PID parameters (K<sub>p</sub>, K<sub>i</sub>, and K<sub>d</sub>) are obtained using the modified Firefly Algorithm (FA) algorithm. By modifying beta (MF-beta), Alpha (MF-Alpha), and Beta-Alpha (MF-Beta-Alpha) values, it is expected to obtain better PID tuning results. These modifications can increase the speed and optimize the firefly computing process in performing optimizations compared to standard parameters. It is hoped that at all times, the surface of the solar panel is always in a position perpendicular to the position of the sun.

## METHODS

### Parameters

Photovoltaic (PV) is the load of the solar tracking system used so that the PV position is always perpendicular to the sun. The gear transmission system is a spur gear consisting of two gears: the M1B12 model (number of teeth 12, mass 10 gr) and the M1A20 model (number of teeth 120, mass 1.32 kg). NPS50W: dimensions of 637 x 545 x 35 mm. The DC motor parameters are presented in Table 1 [15].

Table 1. DC Motor Parameters

Parameter	Value	Parameter	Value
J	3.2284e-6 kg.m <sup>2</sup>	kt	0.0274 Nm / Amp
b	3.5077e-6 Nms	R	4 Ω
kb	0.0274 Vsec / rad	L	2.75e-6 H
J1	2.2642e-3 kg.m <sup>2</sup>	J2	2.22231e3 kg.m <sup>2</sup>
JT1	2.3185e-3 kg.m <sup>2</sup>	JT2	2.22774e3 kg .m <sup>2</sup>

### Transfer Function DC Motor Uncontrolled

The Laplace transform is obtained as (1) by derivation of the motor model.

$$LsI(s) + RI(s) = V(s) - Ks\theta(s) \quad (1)$$

Transfer Function DC Motor without load:

$$\frac{\theta(s)}{V(s)} = \frac{K}{s((J_s + b)(L_s + R) + K^2)} \quad (2)$$

$$\frac{\theta(s)}{V(s)} = \frac{0.00274}{2.384 \times 10^{-9} s^3 + 0.0003467 s^2 + 0.0007647308 s} \quad (3)$$

### Transfer Function Horizontal Axis

The value of the photovoltaic load torque is taken from the moment of inertia of the solar cell panel multiplied by the acceleration of the turning angle. The acceleration of the rotary angle comes from the acceleration of the gear-1 angle. Moment of inertia horizontal rotary axis solar cell panel [15].

$$J_1 = \frac{1}{2} m_{pv} L^2 \left( \frac{N_2}{N_1} \right)^2 \text{ [kg. m}^2\text{]} \quad (4)$$

Horizontal rotary axis sun inertia moment:

$$J_{T1} = J_{st} + J_1 \text{ kg. m}^2 \quad (5)$$

$$\frac{\theta(s)}{V(s)} = \frac{K}{s((J_{T1}s + b)(L_s + R) + K^2)} \quad (6)$$

Horizontal rotary axis sun tracking Transfer Function:

$$\frac{\theta(s)}{V(s)} = \frac{0.00274}{3.289 \times 10^{-9} s^3 + 0.0004783 s^2 + 0.0007647308 s} \quad (7)$$

### Transfer Function Vertical Axis

The acceleration of the rotary angle comes from the acceleration of the gear-2 angle [16]. Moment of inertia of the vertical rotating-axis solar cell panel:

$$J_1 = \frac{1}{2} m_{pv} (L^2 + W^2) \left( \frac{N_2}{N_1} \right)^2 \text{ [kg. m}^2\text{]} \quad (8)$$

The moment of inertia of the vertical rotating Axis PV solar tracker.

$$J_{T2} = J_{st} + J_2 \text{ [kg. m}^2\text{]} \quad (9)$$

$$\frac{\theta(s)}{V(s)} = \frac{K}{s((J_{T2}s + b)(L_s + R) + K^2)} \quad (10)$$

Vertical axis rotary sun tracking transfer function:

$$\frac{\theta(s)}{V(s)} = \frac{0.00274}{2.384 \times 10^{-9} s^3 + 0.0003467 s^2 + 0.00075076 s} \quad (11)$$

The design of the PV control is depicted in Figure 1.

### Firefly Algorithm (FA)

The FA method is often used in system optimization, some of which are used in electric power system optimization. This method has proven its reliability in DC motor rotation optimization, vehicle steer control, micro-hydro frequency control and other system optimizations.



Figure 1. Design of Two Axis solar tracking PV control

Furthermore, this method provides a better understanding of the novel met heuristics from Firefly Algorithm (FA) for the limited continuous optimization task. This method is inspired by the social behavior of fireflies and the phenomenon of bioluminescent communication. The basic steps of the firefly algorithm can be summarized as pseudo-code [17][18]. Data on the standard FA parameters used are listed in [Table 2](#).

Table 2. FA parameters

FA Parameters	Value
Dimension	3
Number of fireflies	50
Maximum iteration	50
Kp_fa	0 – 500
Ki_fa	0 – 100
Kd_fa	0 – 100

### Determines Beta for Firefly

This study uses the ideal firefly determination in photovoltaic by changing the value of the bet. The beta value is changed every step the results are taken, then increased again, and the results are taken. Beta determination is taken from 0.1 up to 0.9.

### Modeling

The FA parameter data in [Table 1](#) is used as a parameter of the program's FA parameters [19]. For example, the design PID Controller for Dual-axis simulation is shown in [Figure 2](#).

### RESULTS AND DISCUSSION

Firefly Algorithm (FA) is widely used in control system optimization. Three FA parameters are used in the system running the program. Beta is used to determine Firefly's movement speed, Alpha is used for movement flexibility, and Gamma is used for more complex constraints or problems. This study uses the ideal firefly determination in photovoltaic by changing the value of the bet. The beta value is changed every step the results are taken, then increased again, and the results are taken. Beta determination is taken from 0.1 up to 0.9 [20]. Block Determination Beta diagram on Firefly can be seen in [Figure 3](#).

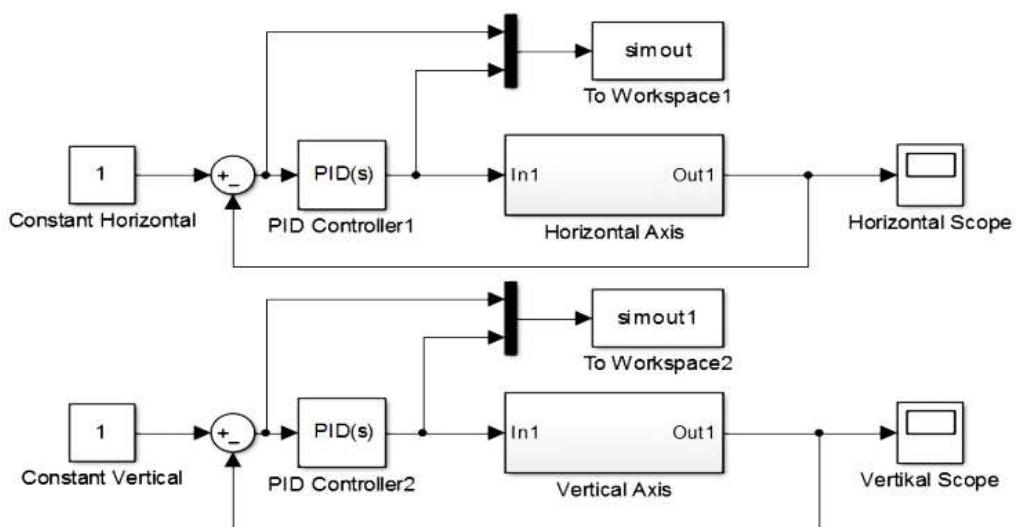


Figure 2. Design-Simulation of PID-Controller for Dual Axis controller

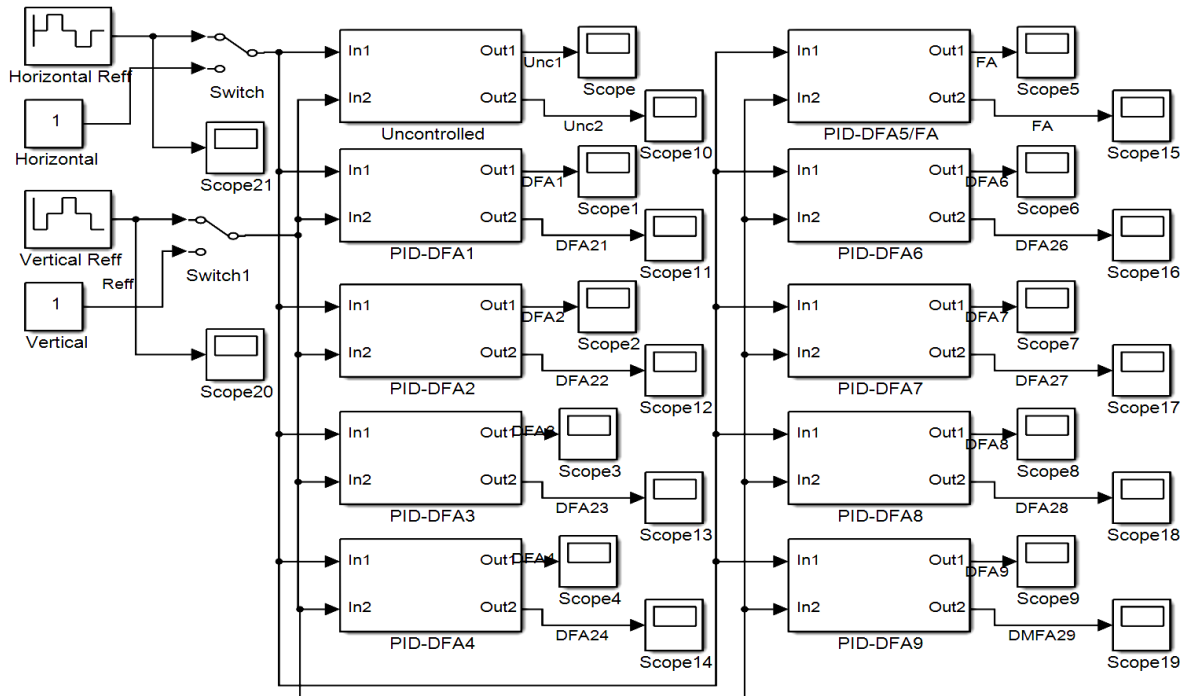


Figure 3. Block diagram of Beta Determination on Firefly

### Horizontal Axis

From the results of 10 models of horizontal axis control, the PID constants ( $K_p$ ,  $K_i$ , and  $K_d$ ) are different from ITAE or Lightest on the same Firefly. With the different constant values of  $K_p$ ,  $K_i$ , and  $K_d$ , the values of overshoot, undershot, and settling time are slightly different. The horizontal axis simulation results can be seen in Figure 4.

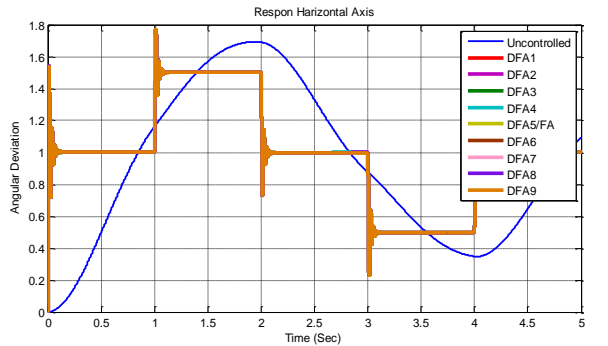
The overshoot value, undershot horizontal Axis, can be seen in Table 3. In Horizontal Axis, by changing the Beta value from 0.1 to 0.9, the values of overshoot, undershot, and settling time varies. Searching for PID constants by DFA obtained difference values that vary with the same ITAE (0.0973) with different PID constant values ( $K_p$ ,  $K_i$ , and  $K_d$ ). From the differences in the constants  $K_p$ ,  $K_i$ , and  $K_d$ , there is a small difference in the value of overshoot and undershot. Table 2 shows that not all firefly modifications produce better values than the firefly original. As evidenced by the value results, DFA5 / FA overshoot is 0.5224, undershot is 0.2658, and settling time is 0.2512. The smallest overshoot value is DFA4 (0.5222), and the biggest overshoot is DFA8 (0.5394). The smallest undershot value is DFA4 (0.2656), and the biggest undershot is DFA8 (0.2789).

The fastest settlement is DFA4 (0.1444), and the slowest is DFA8 (0.2662). This shows that the results of DFA4 (beta = 0.4, alpha = 0.5, and gamma = 0) are the best compared to others.

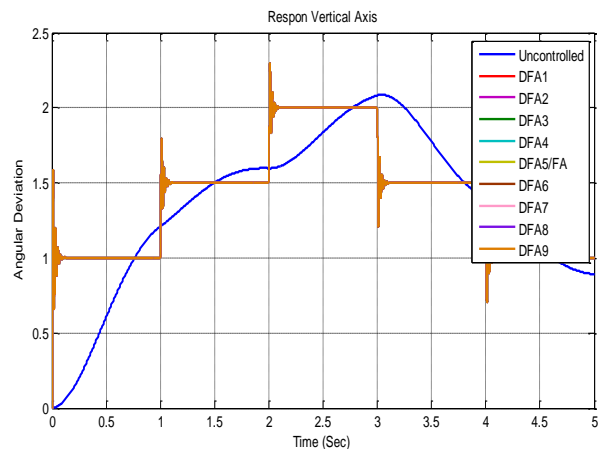
### Vertical Axis

From the results of 10 models controlled by vertical axis control,  $K_p$ ,  $K_i$ , and  $K_d$  values differ from ITAE or Lightest on the same Firefly. With the different constant values of  $K_p$ ,  $K_i$ , and  $K_d$ , the values of overshoot, undershot, and settling time are slightly different. The vertical axis simulation results are shown in Figure 5.

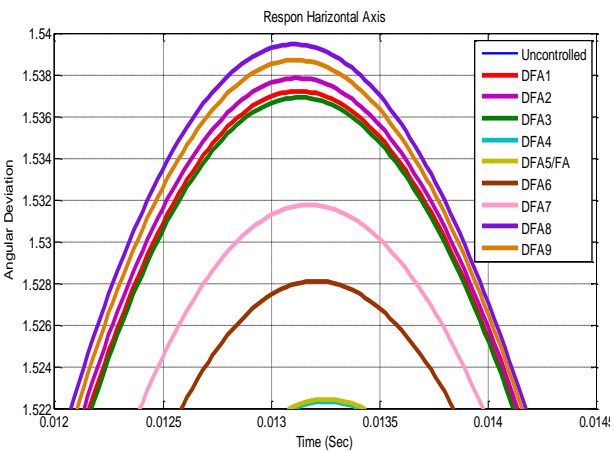
The overshoot value, undershot vertical Axis, can be seen in Table 4. On the Axis vertical, by changing the Beta value to start from 0.1 to 0.9, values of overshoot, undershot, and varying settling time are obtained. Searching for PID constants by DFA obtained difference values that vary with the same ITAE (0.0973) with different PID constant values ( $K_p$ ,  $K_i$ , and  $K_d$ ). From the differences in the constants  $K_p$ ,  $K_i$ , and  $K_d$ , there is a small difference in the value of overshoot and undershot. Table 2 shows that not all modifications of the Firefly Algorithm (DFA5 / FA) produce better value than the firefly original. As evidenced by the value results, FA overshoot is 0.5847, undershot is 0.3365, and settling time is 0.2654.



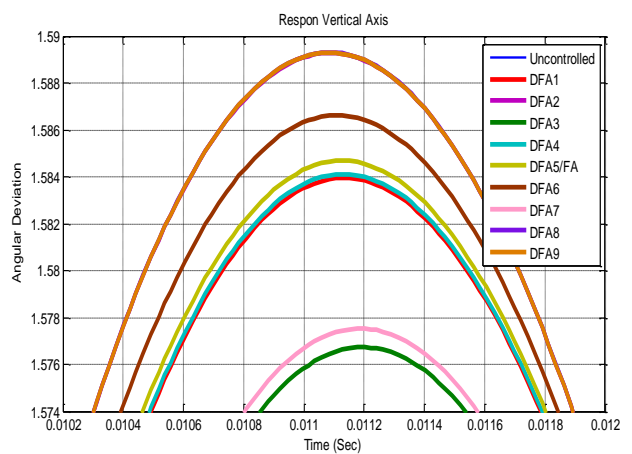
(a) Horizontal axis output results



(a) Vertical axis output results



(b) Overshot Horizontal axis



(b) Overshot Vertical axis

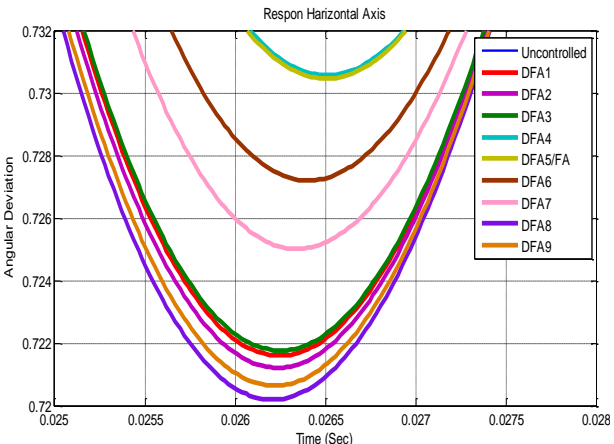


Figure 4. (a) Horizontal axis output results, (b) Overshot Horizontal axis and (c) Undershoot Horizontal axis

The smallest overshoot value is DFA3 (0.5765), and the biggest overshoot is DFA8 (0.5893). The smallest undershoot value is DFA3 (0.3306), and the largest undershoot is DFA8 (0.3403). The fastest settlement is DFA3 (0.1482), and the slowest is DFA8 (0.2691). This shows that the results of DFA3 (beta = 0.3, alpha = 0.5, and gamma = 0) are the best compared to others.

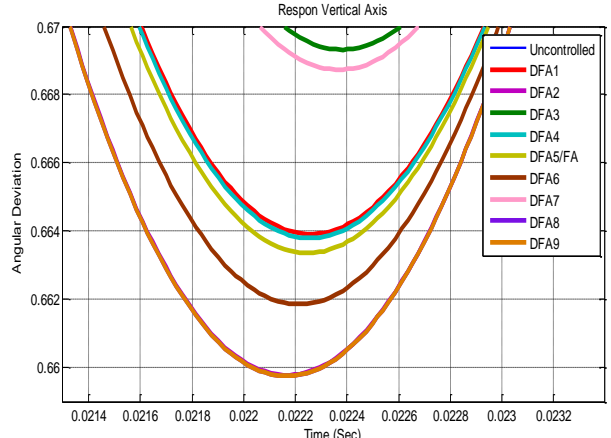


Figure 5. (a) Vertical axis output results, (b) Overshot Vertical axis, (c) Undershoot Vertical Axis

## CONCLUSION

The analysis results obtained optimal performance of the solar tracker with optimal PID parameter tuning. Using the modified firefly method makes the system performance more

optimal than the standard firefly method. From the simulation results, it can be concluded that; by changing the Beta value from 0.1 to 0.9. From the results of 10 models, it was found that the PID constant values were varied. On the horizontal Axis, the best results are if the Beta is given at 0.4 and the worst result is if the Beta is given at 0.8. On the vertical Axis, the best results if the Beta is given at 0.3 and the worst result if Beta is given at 0.8.

## REFERENCE

[1] Suyanto, Soedibyo and A. A. Firdaus, "Design and simulation of Neural Network Predictive Controller pitch-angle in permanent magnetic synchronous generator wind turbine variable pitch system," *2014 The 1st International Conference on Information Technology, Computer, and Electrical Engineering*, 2014, pp. 346-350, doi: 10.1109/ICITACEE.2014.7065769.

[2] C. F. Abe, J. B. Dias, G. Notton and P. Poggi, "Computing Solar Irradiance and Average Temperature of Photovoltaic Modules From the Maximum Power Point Coordinates," in *IEEE Journal of Photovoltaics*, vol. 10, no. 2, pp. 655-663, March 2020, doi: 10.1109/JPHOTOV.2020.2966362.

[3] D. Lin, X. Li, S. Ding and Y. Du, "Strategy comparison of power ramp rate control for photovoltaic systems," in *CPSS Transactions on Power Electronics and Applications*, vol. 5, no. 4, pp. 329-341, Dec. 2020, doi: 10.24295/CPSSTPEA.2020.00027.

[4] S. A. Nabavi, N. H. Motlagh, M. A. Zaidan, A. Aslani and B. Zakeri, "Deep Learning in Energy Modeling: Application in Smart Buildings with Distributed Energy Generation," in *IEEE Access*, vol. 9, pp. 125439-125461, 2021, doi: 10.1109/ACCESS.2021.3110960.

[5] A. A. Firdaus, R. T. Yunardi, E. I. Agustin, T. E. Putri, and D. O. Anggriawan, "Short-term photovoltaic power forecasting using Jordan recurrent neural network in Surabaya," *Telkomnika (Telecommunication Computing Electronics and Control)*, vol. 18, no. 2, pp. 1089-1094, April 2020, doi: 10.12928/TELKOMNIKA.v18i2.14816.

[6] P. A. Østergaard, N. Duic, Y. Noorollahi, and S. A. Kalogirou, "Recent advances in renewable energy technology for the energy transition," *Renewable Energy*, vol. 179, pp. 877-884, 2021, doi: 10.1016/j.renene.2021.07.111Get rights and content

[7] H. Tchakounté, C. B. N. Fapi, M. Kamta, Haman-Djalo and P. Woaf, "Performance Comparison of an Automatic Smart Sun Tracking System Versus a Manual Sun Tracking," *2020 8th International Conference on Smart Grid (icSmartGrid)*, 2020, pp. 127-132, doi: 10.1109/icSmartGrid49881.2020.9144829.

[8] K. Charafeddine and S. Tsyruk, "Automatic Sun-Tracking System," *2020 International Russian Automation Conference (RusAutoCon)*, 2020, pp. 191-195, doi: 10.1109/RusAutoCon49822.2020.9208086.

[9] A. -H. I. Mourad, H. Shareef, N. Ameen, A. H. Alhammadi, M. Iratni and A. S. Alkaabi, "A state-of-the-art review: Solar trackers," *2022 Advances in Science and Engineering Technology International Conferences (ASET)*, 2022, pp. 1-5, doi: 10.1109/ASET53988.2022.9735074.

[10] M. R. Nugraha and A. Adriansyah, "Development of a solar radiation sensor system with pyranometer," *International Journal of Electrical and Computer Engineering (IJECE)*, vol. 12, no. 2, pp. 1385-1391, 2022, doi: 10.11591/ijece.v12i2.pp1385-1391

[11] M. A. Shameli, A. Fallah, and L. Yousefi, "Developing an optimized metasurface for light trapping in thin-film solar cells using a deep neural network and a genetic algorithm," *Journal of the Optical Society of America B*, vol. 38, no. 9, pp. 2728-2735, 2021, doi: 10.1364/JOSAB.432989

[12] M. S. Ahmad and A. Ahmad, "Hybrid PSO-DE technique to optimize energy resource for PV system," *International Journal of Electrical Engineering and Technology (IJEET)*, vol. 12, no. 6, pp. 128-139, 2021, doi: 10.34218/IJEET.12.6.2021.014

[13] A. A. Firdaus, R. T. Yunardi, E. I. Agustin, S. D. N. Nahdliyah, and T. A. Nugroho, "An improved control for MPPT based on FL-PSO to minimize oscillation in photovoltaic system," *International Journal of Power Electronics and Drive Systems*, vol. 11, no. 2, pp. 1082~1087, June 2020, DOI: 10.11591/ijpeds.v11.i2.pp1082-1087

[14] M. R. Djalal and F. Faisal, "Design of optimal PID controller for three phase induction motor based on Ant Colony Optimization," *SINERGI*, vol. 24, no. 2, pp. 125-132, 2020, doi: 10.22441/sinergi.2020.2.006

[15] M. Ali, H. Nurohmah, Budiman, J. Suharsono, H. Suyono, and M. A. Muslim, "Optimization on PID and ANFIS Controller on Dual Axis Tracking for Photovoltaic Based on Firefly Algorithm," in *2019 International Conference on Electrical, Electronics and Information Engineering (ICEEIE)*, 2019, pp. 1-5, doi: 10.1109/ICEEIE47180.2019.8981428.

[16] A. Adhim and A. Musyafa, "Optimization of PID Controller Based on PSO for Photovoltaic Dual Axis Solar Tracking in Gresik Location – East Java," *International Journal of Engineering & Technology IJET-IJENS*, vol. 16, no. 1, pp. 65–72, 2016.

[17] M. Ravindrababu, G. Saraswathi, and K. R. Sudha, "Design of firefly based power system stabilizer based on pseudo spectrum analysis," *International Journal on Electrical Engineering and Informatics*, vol. 9, no. 1, pp. 195–206, 2017, doi: 10.15676/ijeei.2017.9.1.14.

[18] K. R. Kumar, P. P. Raj, and P. R. Kumar, "Firefly Algorithm based Pseudo-Orthogonal codes for reducing sidelobes and electromagnetic interference.," in *15th International Conference on Electromagnetic Interference and Compatibility, INCEMIC 2018*, 2019, doi: 10.1109/INCEMIC.2018.8704576.

[19] M. Ali, Muhlasin, H. Nurohmah, A. Raikhani, H. Sopian, and N. Sutantra, "Combined ANFIS method with FA, PSO, and ICA as Steering Control Optimization on Electric Car," in *2018 Electrical Power, Electronics, Communications, Controls and Informatics Seminar (EECCIS)*, 2018, pp. 299–304, doi: 10.1109/EECCIS.2018.8692885.

[20] X. S. Yang, "Analysis of firefly algorithms and automatic parameter tuning," in *Emerging Research on Swarm Intelligence and Algorithm Optimization*, IGI Global, UK, 2014, pp. 36–49, doi: 10.4018/978-1-4666-6328-2.ch002

Table 3. Horizontal axis output results

	DFA1	DFA2	DFA3	DFA4	DFA/FA	DFA6	DFA7	DFA8	DFA9
Beta	0.1	0.2	0.3	0.4	0.5	0.6	0.7	0.8	0.9
Lightbest	0.0973	0.0973	0.0973	0.0973	0.0973	0.0973	0.0973	0.0973	0.0973
ITAE	0.0973	0.0973	0.0973	0.0973	0.0973	0.0973	0.0973	0.0973	0.0973
Kp	411.1302	499.4173	294.5546	413.6636	423.1084	455.1539	307.3056	500.0000	500.0000
Ki	35.2884	34.8023	58.9795	43.5902	44.7332	37.3888	51.3838	9.5872	0.0000
Kd	100.0000	100.0000	100.0000	100.0000	100.0000	100.0000	100.0000	100.0000	100.0000
Overshot	0.5377	0.5379	0.5368	0.5222	0.5224	0.5282	0.5317	0.5394	0.5386
Undershoot	0.2783	0.2785	0.2781	0.2656	0.2658	0.2736	0.2747	0.2789	0.2787
Settling time	0.1843	0.1931	0.1963	0.1444	0.2512	0.2554	0.1521	0.2662	0.2641

Table 4. Vertical axis simulation results

	DFA1	DFA2	DFA3	DFA4	DFA/FA	DFA5/FA	DFA6	DFA7	DFA8	DFA9
Beta	0.1	0.2	0.3	0.4	0.5	0.6	0.7	0.8	0.9	0.9
Lightbest	0.0973	0.0973	0.0973	0.0973	0.0973	0.0973	0.0973	0.0973	0.0973	0.0973
ITAE	0.0973	0.0973	0.0973	0.0973	0.0973	0.0973	0.0973	0.0973	0.0973	0.0973
Kp	467.5148	476.5024	463.4701	255.4461	257.6211	336.4739	388.2570	500.0000	489.5432	489.5432
Ki	42.4961	56.4522	10.4465	56.5889	8.7630	48.6185	56.9651	80.4220	23.6364	23.6364
Kd	100.0000	100.0000	100.0000	100.0000	100.0000	100.0000	100.0000	100.0000	100.0000	100.0000
Overshot	0.5838	0.5839	0.5765	0.5841	0.5847	0.5865	0.5776	0.5893	0.5894	0.5894
Undershoot	0.3362	0.3425	0.3306	0.3363	0.3365	0.3381	0.3308	0.3403	0.3404	0.3404
Settlingtime	0.1972	0.1961	0.1482	0.2564	0.2654	0.1862	0.1863	0.2691	0.2713	0.2713